Arabian Journal of Chemical and Environmental Research

Vol. 08 Issue 01 (2021) 114–132

Cowpea husk adsorbent for the removal of crystal violet dye from aqueous solution

Abdullahi Muhammad Ayuba* and Bridget Idoko

[1]*Department of Pure and Industrial Chemistry, Faculty of Physical Sciences, Bayero University, PMB 3011, Kano, Nigeria.*

Received 11 January 2021, Revised 05 February 2021, Accepted 06 February 2021

Abstract

Cowpea husk (CPH) was used as a low cost, effective and environmental friendly adsorbent for the removal of crystal violet dye from wastewater. Batch adsorption studies were conducted under various optimized experimental conditions such as agitation time (90minutes), dye concentration (50mg/l), adsorbent dose (0.1g) and pH (6) respectively. The adsorbent surface was characterized through Fourier Transform Infrared Spectroscopy (FTIR) and Scanning Electron Microscopy (SEM) techniques, while the physical properties (bulk density, moisture content and pore volume) of the adsorbent were determined using standard reported methods. The adsorption data were analysed using Langmuir, Freundlich and Temkin isotherm models to propose the mechanism of the adsorption process. Equilibrium data fitted well to Langmuir isotherm with maximum adsorption capacity of 153.85mg/g and R^2 value of 0.907 which is almost unity signifying a mechanism of chemical adsorption. Adsorption kinetic data were verified using pseudo first order, pseudo second order, Elovich and intra-particle diffusion models. The kinetic data were found to fit well with pseudo second order model. Thermodynamics of the adsorption process indicates the process to be feasible and spontaneous. This study recommends that CPH could be employed as a low-cost adsorbent as alternative to other expensive adsorbents for the removal of dyes from wastewater.

Keywords: Adsorption, kinetic, thermodynamic, Isotherms, Crystal Violet

*Corresponding author.
E-mail address: ayubaabdullahi@buk.edu.ng

ISSN : 2458-6544 © 2021 ;www.mocedes.org. All rights reserved.

1. Introduction

Effluents from the textile, paper, and pulp industries contaminate the environment and therefore, before discharging wastewater from dyeing industries into natural water streams, there is need for its treatment. The adsorption technique for the removal of dyes from effluents is cheap, safe and the most widely method [1-5]. Most types of dyes used in textile industries are either the direct, reactive, acid and/or basic dyes. Basic dyes are the brightest class of soluble dyes used by textile industries. Most of these dyes present acute problems to the ecological system as they are considered toxic and have carcinogenic properties, which make the water inhibitory to aquatic life. Due to their chemical structure, dyes are reported to possess a high potential to resist degradation on exposure to light and water [6]. The main sources of wastewater generated by the textile industry originate from the washing and bleaching of natural fibres and from the dyeing and finishing steps given the great variety of fibers, upon which dyes are used. These processes generate wastewater of great chemical complexity and diversity, which are not adequately treated in conventional wastewater treatment plants [7].

Crystal violet (CV) is a well-known cationic dye among the various available dyes, which has variety of applications such as a biological stain, dermatological agent, additive to poultry feed to inhibit propagation of mould, intestinal parasites and fungus, textile dying and paper printing, veterinary medicine, etc. [8]. However, crystal violet is a mutagen and mitotic poison and also toxic to mammalian cells. Effluents of textile and paper printing industries contain crystal violet dye in large quantity that must be treated to reduce its impact on environment [9]. Alternative adsorbents of plant origin investigated for the removal of organic contaminants are Bambara groundnut hulls [10], *Vigna subterranean* (L.) Verdc Hull [11], *Adansonia digitata* [12], *Balanites aegyptiaca* [13], *Zizyphus mauritiana* [14], among others. In this work, low cost cowpea husk was chosen to investigate its adsorption capacity for crystal violet present in aqueous solution. The effects of various parameters such as contact time and adsorbent mass on the adsorption efficiency of crystal violet were studied using the batch technique. The kinetics of crystal violet adsorption on cowpea husk was analyzed by pseudo first order, pseudo second order and Elovitch kinetic models. Experimental equilibrium data were fitted to the Langmuir, Freundlich and Temkin isotherm equations to determine the best-fit isotherm equation.

2. Materials and methods

2.1 Adsorbent collection and preparation

The cowpea (*Vigna unguiculata*) husk (CPH) was obtained from a local market in Kano, Nigeria. The husk obtained after removing the seed from the pod was washed and air dried by removing the bean seeds. CPH was first washed with water to remove dirt from its surface and subsequently dried at 105^{o}

C for 24 hrs in an oven to remove the moisture content. The dried CPH was ground into small pieces and sieved to the desired particle size of 2 mm, stored in an airtight container and labelled R-CPH (Raw Cowpea Husk) (Figure 1).

Figure 1. Ground powder of raw cowpea husk

2.2 Preparation of crystal violet solution

In the present investigation, water-soluble crystal violet (Figure 2, molecular formula $C_{25}N_3H_{30}Cl$, molecular weight 407.979 g mol^{-1}) was obtained from Merck, and a 0.1M stock solution was prepared in distilled water. Solutions of desired concentrations of the adsorbate were prepared from the stock solution, where distilled water was used for necessary dilutions. All reagents used were of analytical grade. The concentration of the residual un-adsorbed CV dye was measured at λ_{max} = 590.3 nm using UV–visible spectrophotometer (Model Hitachi 2800).

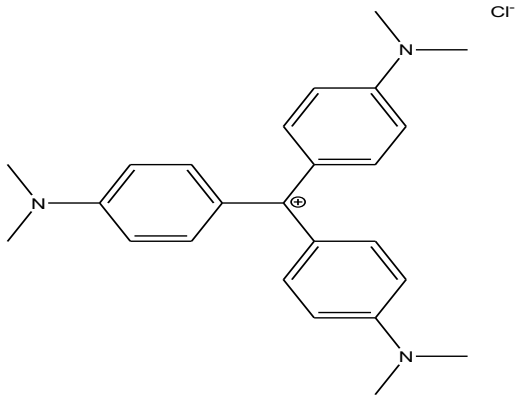

Figure 2. Structure of crystal violet (Tris(4-(dimethylamino)phenyl)methylium chloride)

2.3 Characterization of the adsorbent

This raw material is well characterized by Fourier Transform Infrared Spectroscopy (FTIR) and Scanning Electron Microscopy (SEM) techniques, while the physical properties (bulk density, moisture content and pore volume) of the adsorbent were determined using standard reported methods.

(a) Determination of bulk density

The bulk density of R-CPH was determined using Archimedes' principle by weighing 10cm^3 measuring cylinder before and after filling with the samples. The measuring cylinder was then dried and the sample was packed inside the measuring cylinder, levelled and weighed. The weight of the sample packed in the measuring cylinder was determined from the difference in weight of the filled and empty measuring cylinders. The volume of water in the cylinder was determined by taking the difference in weight of the empty and water filled measuring cylinder. The bulk density was determined using the equation (1) [8-9]:

$$\text{Bulk density} = \frac{W_2 - W_1}{V} \quad (1)$$

Where; w_1 is weight of empty measuring cylinder, w_2 is weight of cylinder filled with sample and v is volume of the cylinder.

(b) Moisture content determination

This was done by the gravimetric method as described by AOAC [15] and others [8-9]. 15g of RCPH was weighed and put into a weighed crucible. The crucible and its contents were dried in the oven at 130^{o}C for 1 hour in the first instance. It was cooled in a desiccator and reweighed. The weight was recorded while the sample was returned to the oven for further drying. Sample was heated for the second time at 100°C for 30mins, cooled in a desiccator and weighed again. The procedure was repeated several times at the same temperature for 30mins intervals until a constant weight was obtained. The percentage moisture content of each sample was calculated using equation (2):

$$\% \text{ moisture content} = \frac{W_2 - W_3}{W_2 - W_1} \times 100 \quad (2)$$

Where; w_1 is weight of crucible, w_2 is initial weight of crucible with sample, w_3 is final weight of crucible with sample.

(c) Pore (Void) volume determination

In order to determine the pore volume of the R-CPH, 2.0 g of the sample was immersed in water and boiled for 15 min. After the air in the pores had been displaced, the sample was superficially dried and reweighed. The increase in weight divided by the density of water gave the pore volume [8-9, 15].

(d) Scanning electron microscopy (SEM)

The surface morphological changes of R-CPH samples were investigated using Scanning Electron Microscope (Phenom World Eindhoven). Scanned micrographs of R-CPH before and after adsorption were taken at an accelerating voltage of 15.00 kV and x500 magnification.

(e) Fourier transform infrared (FT-IR) analysis

FTIR analysis of R-CPH before and after adsorption was carried out using Cary 630 Fourier Transform Infrared Spectrophotometer Agilent Technology. The resulting residue collected was dried for FTIR analysis. The analysis was carried out by scanning the sample through a wave number range of 650 – 4000 cm^{-1}; 32 scans at 8cm^{-1}resolution.

2.4 Batch adsorption experiments

Batch experiments were carried out to determine the optimum conditions for the equilibrium adsorption of crystal violet onto raw cowpea husk adsorbent. The results obtained after the optimization experiments (0.1g of R-CPH, 90 minutes' contact time, solution pH of 6) were used to conduct the batch adsorption experiments. Each of these systems was separately run in a 250 cm^3 conical flask differently at (30 - 60)^{0}C respectively. The conical flasks were covered during the equilibration period and placed on a temperature-controlled tightly Innova 4000 incubator shaker for the earlier reported period. After reaching adsorption equilibrium, the content was filtered through Whatman No 1 filter paper. The filtrate was analysed using Perkin-Elemer Uv-visible spectrophotometer at maximum absorbance wavelength of 590.3nm [16]. The extent of adsorption was calculated using equations (3) and (4) respectively.

$$q_e = \frac{(Co-Ce)}{m} \times v \quad (3)$$

$$R_{em}(\%) = \frac{(Co-Ce)}{Co} \times 100 \quad (4)$$

Where q_e is the adsorption capacity (mg/g), R_{em} is the percentage adsorption, C_o and C_e are the initial and final equilibrium concentration (mg/l) of crystal violet solution, v is the volume of crystal violet solution (L), and m is the mass (g) of the adsorbent.

3. Results and discussion

3.1 Adsorbent surface characterization

a) FTIR Spectroscopy

In the FTIR spectrum as shown in **Figure 3** of R-CPH before adsorption of CV, there is a broad adsorption band at 3279 cm^{-1} which is assigned to –OH of hydroxyls, and also prominent peaks at 2918cm^{-1} assigned to C – H bonds of methyl and methylene groups [17]. The presence of OH group and carbonyl group is attributed to the presence of carboxylic acids group present in the adsorbents. The stretching of the C-O group to aromatic ring is attributed to the signal at 1104cm^{-1}. The hydroxyl, carboxyl and carboxylic acid are important adsorption site [18].

After adsorption, there was a shift and broadening of adsorption peaks. The shift of the OH peak from 3272cm^{-1} to 3320cm^{-1} indicates the involvement of the hydroxyl groups in the adsorption. Other shifts

involving that of C=O (1630 to 1630) cm^{-1}, O=C-O (1728 to 1722) cm^{-1}, C=C (1547 to 1525) cm^{-1}, C-O (1104 to 1100) cm^{-1} are indicators that there is an interaction between the surface of R-CPH and the CV molecules through adsorption. The result on the **Table 1** of the FTIR spectrum (**Figure 3)** shows the participation of carbonyl and hydroxyl groups of the adsorbent as active binding site for adsorption of CV [19]. However, shift in bands and changes in wavelength between the before and after adsorption of samples indicate that the nature of the adsorption of the dye onto the adsorbent must likely be through physical means involving vander Waals forces of attraction.

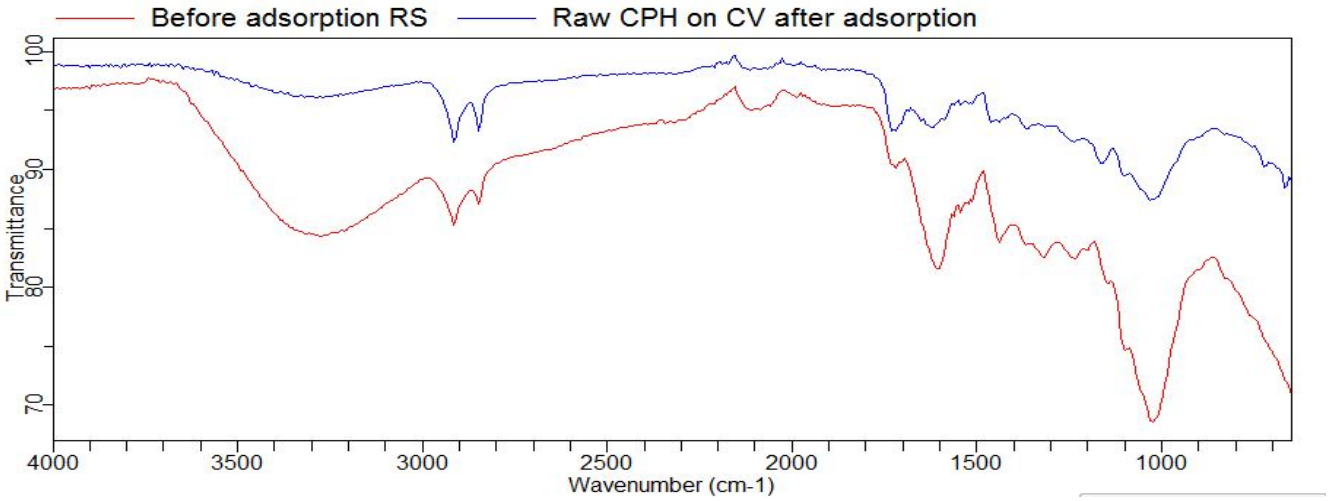

Figure 3. FTIR spectral of R-CPH before and after adsorption of CV

Table 1. Different functional groups recognized before and after adsorption of CV onto R-CPH

Functional Group	Wavelength class range (cm^{-1})	Before adsorption (cm^{-1})	After adsorption (cm^{-1})
O-H stretch	3300-3400	3279	-
C-H stretch	2950-2800	2918	2918
C=O	1900-1600	1610	1630
Carboxylic group	1690- 1760	1722	1728
C=C aromatics	1500- 1700	1547	1525
C-O stretch	1080- 1300	1100	1104

b) Scanning electron microscopy (SEM)

Scanned micrographs of adsorbents before and after adsorption of CV were taken at an accelerating voltage of 15.00 kV and x500 magnification. The SEM of R-CPH before adsorption (Figure 4a) shows a moderately rough surface which is characterized with defects made of cracks and cavities and probably with presence of adhering particles which may be dust or other impurities [20]. The micrograph of R-

CPH after adsorption of CV (Figure 4b) shows depositions of adsorbed dyes in smooth regular formations on the surfaces, with most of cracks and cavities fill up with the adsorbed CV dye. That is an evidence of the interaction between the CV dye and the R-CPH surface.

3.2 Physical Properties of the R-CPH

Some of the physical properties of the adsorbent are presented in **Table 2**. The values of the moisture content, pore volume and the bulk density of the adsorbent were found to reveal that it had good adsorptive properties. Low moisture content, high pore volume are properties that have been reported to enhance adsorption for species which are either organic and inorganic in nature to a large extent [21].

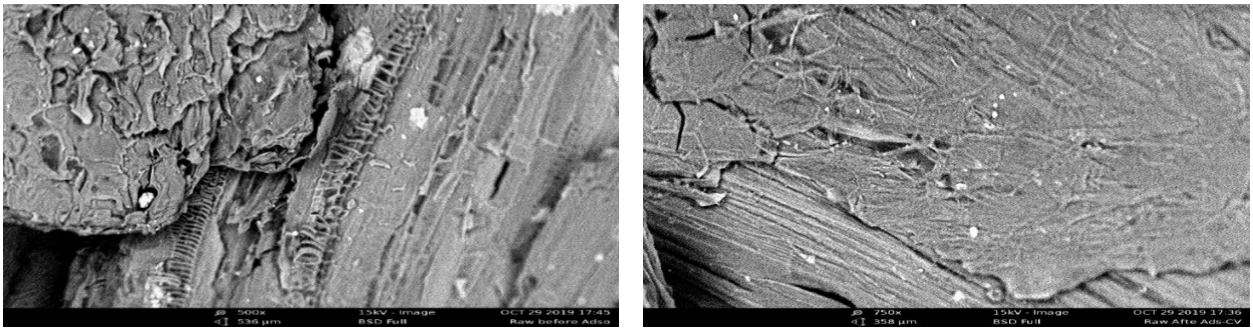

(a) (b)

Figure 4. SEM Micrograph of R-CPH (a) before and (b) after adsorption of CV

Table 2: Physical Properties of adsorbent (Raw Cowpea husk) used

Adsorbent	Moisture Content	Density	Pore Volume
R-CPH	14.5%	0.323g/cm^3	1.25cm^3

3.3 Parameter optimizations and batch adsorption

Figure 5a shows the effect of the quantity of R-CPH used on the adsorption of crystal violet in which the amount of adsorbent was varied from 0.1 to 0.8 g while the dyes concentration was fixed at 50 mg/L. The net quantity of the adsorbate removed increased with increasing mass of R-CPH which is attributed to an increase in the adsorptive surface area and the availability of more active binding sites. The net equilibrium amount adsorbed however is an expression of the efficiency of an adsorbent which may not show increase in the amount adsorbed per unit mass as the adsorbate dose increases [22]. The amount of crystal violet dye adsorbed per unit mass of R-CPH decreased as the R-CPH dosage was increased from 0.1 – 0.6 g. This may be due partly to the inaccessibility of the active sites and partly to overlapping or aggregation of adsorption sites as the adsorbate dose increases [22]. Thus, with increasing adsorbent mass, the amount of dye adsorbed onto unit mass of adsorbent gets reduced, thus causing a decrease in adsorption capacity (qe) value with increasing adsorbent mass concentration (with optimal at 0.1g).

Figure 5b indicates the effect of contact time on adsorption of crystal violet onto R-CPH which was studied at 50mg/l concentration at initial pH 8 at 298 K. When the system reaches adsorption equilibrium; no further net adsorption occurs. The time at which adsorption equilibrium occurs was determined from the plot of dyes uptake versus contact time (min). From the experimental data, the process of adsorption reaches the equilibrium state after approximately 90 min for the crystal violet. Further, the adsorption proceeds at a lower rate and finally no significant adsorption are noted beyond 60 min. In industry, this contact time is very important for process optimization. The fast sorption of CV at the beginning sorption time can be attributed to the availability of a large number of vacant sites on the adsorbent surface, which was filled up by the dye molecules [24].

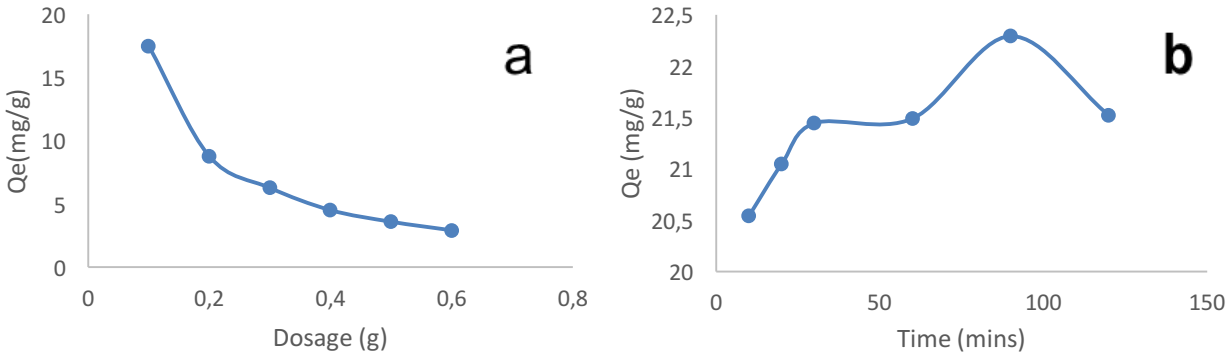

Figure 5. Effect of (a) adsorbent dosage and (b) contact time on the adsorption of CV onto the R-CPH

Figure 6a shows the effect of initial CV concentration on the adsorption rate. The experiment was carried out with fixed R-CPH dose (0.1 g/l) at room temperature. The adsorption capacity was found to increase (23.66 - 244.18) mg/g when the dye concentration was increased (50 – 500) mg /L. The increase in dye concentration enhanced the interaction between the dye and R-CPH providing necessary driving force to overcome the resistance to mass transfer of dye [25]. Therefore, rate of adsorption and hence dye uptake increased with an increase in dye concentration.

Figure 6b shows the effect of pH on the adsorption of CV onto R-CPH. The pH of the dye solution plays an important role in the whole adsorption process and particularly on the adsorption capacity. pH of solution not only affecting the surface charge of the adsorbent, the degree of ionization of the dyes present in the solution and the dissociation of functional groups on the active sites of the adsorbent, but also the solution dye chemistry [6]. The hydrogen and hydroxyl ions are adsorbed quite strongly, and therefore, the adsorption of other ions is affected by the pH of the solution. It is commonly known fact that at high pH values, cationic dyes are adsorbed due to the negatively charged surface sites of R-CPH. In the present adsorption system, the adsorption capacity of CV is highest at pH 6 with maximum adsorption capacity of 21.23mg/g as shown in Figure 6b. This is in agreement with reports of the adsorption of dyes by other authors [26].

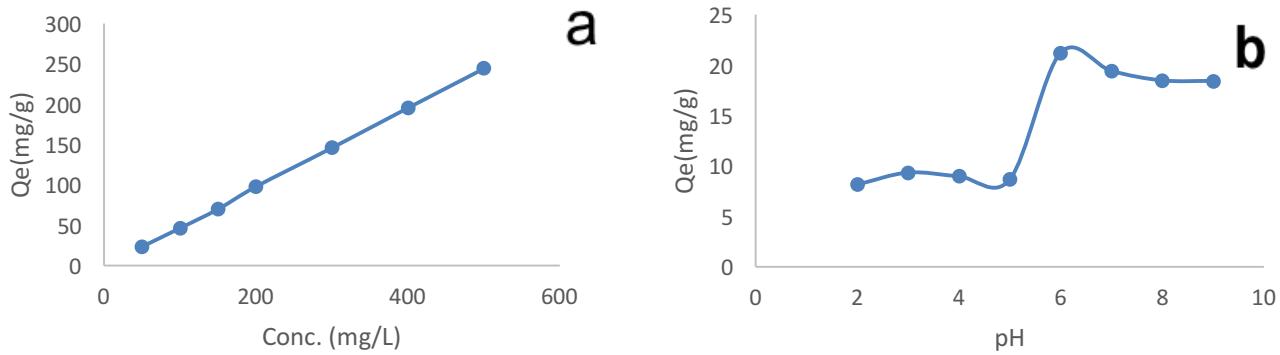

Figure 6. Effect of (a) initial dye concentration (b) pH of the CV adsorption onto R-CPH

3.4 Adsorption kinetics

The data generated during batch adsorption experiments when samples were withdrawn at 10 minutes' interval for a maximum period of 120 minutes was subjected to different kinetic models. This is with an aim of possibly establishing the mechanism of the interaction of the dye with the surface of the adsorbent (R-CPH). The following models were tested, reported and discussed:

(a) The pseudo first-order equation

The pseudo first-order equation is generally expressed as follows [27]:

$$\frac{\partial q_t}{\partial t} = k_1(q_e - q_t) \quad (5)$$

Where q_e and q_t are the adsorption capacity at equilibrium and at time t, respectively (mg/g), k_1 is the rate constant of pseudo first-order adsorption (min^{-1}). After integration and applying boundary conditions $t = 0$ to $t = t$ and $q_t = 0$ to $q_t = q_t$, the integrated form becomes:

$$\log(q_e - q_t) = \log(q_e) - \frac{k_1}{2.303}t \quad (6)$$

The values of $log\ (q_e - q_t)$ were linearly correlated with t. The plot of $log\ (q_e - q_t)$ vs. t gave a linear relationship from which k_1 and q_e were determined from the slope and intercept of the plot respectively (Figure 7a).

(b) The pseudo second-order equation

The pseudo second-order adsorption kinetic rate equation is expressed as in equation (7):

$$\frac{\partial q_t}{\partial t} = k_2(q_e - q_t)^2 \quad (7)$$

Where k_2 is the rate constant of pseudo second-order adsorption ($g \cdot mg^{-1} \cdot min^{-1}$). For the boundary conditions $t = 0$ to $t = t$ and $q_t = 0$ to $q_t = q_t$, the integrated form of equation (7) becomes:

$$\frac{1}{(q_e - q_t)} = \frac{1}{q_e} + k_t \quad (8)$$

This is the integrated rate law for a pseudo second-order reaction.

The equation can be rearranged to obtain equation (9), which has a linear form thus:

$$\frac{t}{q_t} = \frac{1}{K_2\, q_e^2} + \frac{1}{q_e}\ (t) \qquad (9)$$

If the initial adsorption rate, h (mg·g^{-1}·min^{-1}) is;

$$h = k_2 q_e^2 \qquad (10)$$

Then equation (10) becomes

$$\frac{1}{q_t} = \frac{1}{h} + \frac{1}{q_e}(t) \qquad (11)$$

The plot of (t/q_t) and t gave a linear relationship from which q_e and k_1 were determined from the slope and intercept of the plot respectively (Figure 7b).

(c) Elovich equation

The Elovich kinetic model is described by the following relation [28]:

$$q_t = 1/\beta \ln(\alpha\beta) + (1/\beta) \ln t \qquad (12)$$

This model gives useful information on the extent of both surface activity and activation energy for adsorption process. The parameters *(α)* and *(β)* was calculated from the slope and intercept of the linear plot of qt versus ln(t) (Figure 7c).

(d) Intraparticle diffusion equation

The slowest step in an adsorption process is usually taken as the rate determining step. This step is often attributed to pore and intra particle diffusion. Since pseudo first and pseudo second order models cannot provide information on effect of intra particle diffusion in adsorption, intra particle diffusion model can be used. Possibility of involvement of intra particle diffusion model as the sole mechanism was investigated according to Weber–Moris equation [29]:

$$q_e = C + k_{int} t_{\frac{1}{2}} \qquad (13)$$

Where the constant k_{int} (mg/g min^{-1}) is the intra particle diffusion rate and C is the boundary layer thickness. If the rate-limiting step is only due to the intra particle diffusion, then q_t versus $t_{1/2}$ gave a linear plot which passes through the origin (Figure 7d).

Table 3 shows kinetic models for the adsorption of CV onto the adsorbent, R-CPH. The pseudo-second-order kinetic model fits the experimental data quite well; the correlation coefficients values, R^2, all up to almost unity, and the experimental and theoretical uptakes are in good agreement. This was not the case for the other tested kinetic models whose R^2 values are relatively very low. This indicates the applicability of the second-order kinetic model to describe the adsorption process of CV onto the adsorbent, R-CPH.

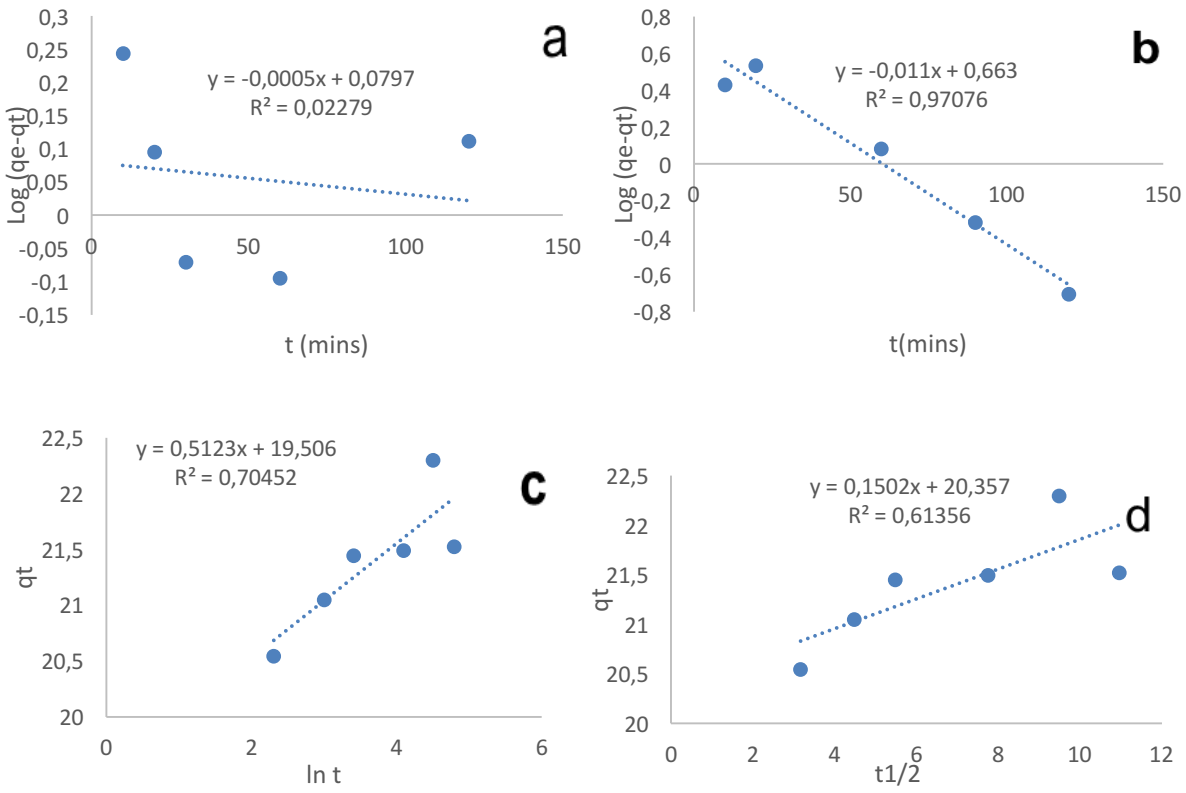

Figure 7. (a) pseudo-first order (b) pseudo-second order (c) Elovich linear (d) Intra particle diffusion plot for adsorption of CV onto R-CPH

Table 3. Kinetic parameters for the adsorption of CV onto R-CPH

Kinetic models		**Parameters**		
Pseudo-first order	q_{eExp}(mg/g)	q_{eCal}(mg/g)	k_1(min^{-1})	R^2
	22.295	0.079	0.001	0.023
Pseudo-second order	q_{eExp}(mg/g)	q_{eCal}(mg/g)	k_2(min^{-1})	R^2
	22.295	21.882	0.083	0.999
Elovich		B	A	R^2
		1.952	5.22	0.705
Intra particle diffusion		k_3	C	R^2
		0.510	20.357	0.614

3.5 Adsorption isotherm models

Three isotherm equations were used to find out the relationship between the equilibrium concentration of the adsorbate in the liquid phase and in the solid phase adsorbent. More importantly, to determine which of the isotherms best describes the adsorption mechanism process. Experimental data were

substituted into the equations and appropriate graphs, constants and other variables were generated for each of the following equations:

(a) Langmuir isotherm

The Langmuir isotherm is described mathematically by equation (14):

$$\frac{1}{q_e} = \frac{1}{Q_o} + \frac{1}{Q_o K L C_e} \quad (14)$$

Where C_e is the equilibrium concentration of adsorbate (mg/L), q_e is the amount of CV adsorbed per gram of the adsorbent at equilibrium (mg/g), Q_o is maximum monolayer coverage capacity (mg/g), K_L is Langmuir isotherm constant (L/mg). The values of q_{max} and K_L were computed from the slope and intercept of the Langmuir plot of $\frac{1}{qe}$ versus $\frac{1}{Ce}$. Thus, a plot of 1/qe versus 1/*C*e gave a straight line of intercept $1/Q_o$ and slope $1/Q_oK_L$ (Figure 8). The plotting of CV molecule adsorbed (1/qe) by R-CPH against the equilibrium concentration of CV molecule (1/Ce) in solution gives the equilibrium isotherm and the values of R_L and K_L were calculated and tabulated in Table 4. The value of the correlation coefficient of R-CPH onto CV indicated that the adsorption of CV molecule fit well into the Langmuir model. The fundamental features of the Langmuir isotherm can be described in terms of separation factor or equilibrium parameter R_L, which is defined by equation (14) [30].

$$R_L = \frac{1}{1+(1+K_L C_O)} \quad (15)$$

Where C_o is the highest initial CV concentration in the solution (mg/L). The result for the separation factor (R_L) for this study is presented in Table 4.

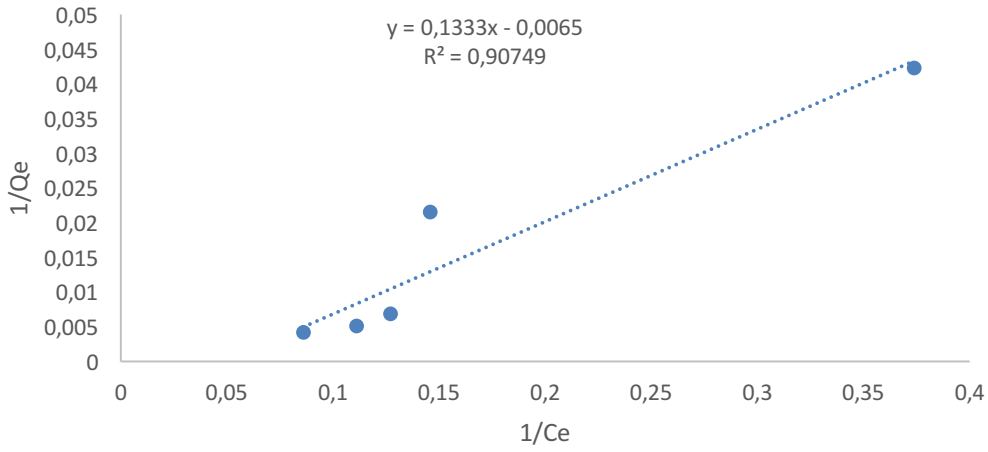

Figure 8. Langmuir adsorption isotherm plot for adsorption of CV onto RCPH

(b) Freundlich isotherm

The equilibrium concentrations of CV dye obtained were subjected to Freundlich equation as shown in equation (16) [31]:

$\log q_e = \log K_f + (1/n) \log C_e$ (16)

Where K_f is a constant indicative of the relative adsorption capacity of the adsorbent and n is adsorption intensity related to the surface heterogeneity. Both K_f and *n* were determined by the linear plot of log q_e versus log C_e (Figure 9). If *n* = 1 then the partition between the two phases are independent of the adsorbate concentration. If a value of 1/*n* is below one, it indicates a normal adsorption process [32]. On the other hand, 1/*n* values above one indicates cooperative adsorption process [33]. The heterogeneity parameter is given by 1/n. The smaller 1/*n*, the greater the expected heterogeneity and the Freundlich expression reduces to a linear adsorption isotherm when 1/*n* = 1. If n lies between one and ten, this indicates a favourable adsorption process [34]. The value of correlation coefficient (R^2 = 0.876) of CV onto R-CPH indicated that the adsorption of CV molecule does not fits very well into the Freundlich Isotherm.

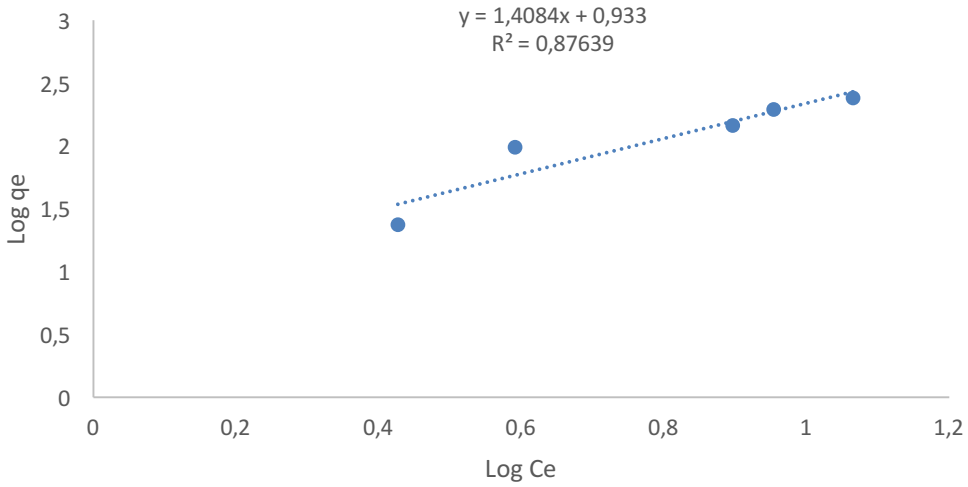

Figure 9. Freundlich adsorption isotherm plot for adsorption of CV onto RCPH

(c) Temkin isotherm

Unlike the Langmuir and Freundlich equations, the Temkin isotherm model considers the interactions between adsorbent material and CV molecule to be adsorbed and is assuming that the free energy of adsorption process is a function of the surface coverage [35-36]**.** In addition, the heat of adsorption of all the adsorbate molecules in the layer decreases linearly due to adsorbent–adsorbate interactions, and the adsorption is characterized by a uniform distribution of the binding energies, up to some maximum binding energy [37]**.** It is expressed by equation (17):

$$q_e = \frac{RT}{b_T} lnA_T + (\frac{RT}{b}) lnC_e \quad (17)$$

Where Temkin constant B = RT/b is related to the heat of adsorption, R is the gas constant (J/mol *K), T* the temperature (K), b the variation of the adsorption energy (J/mol) and b_T the equilibrium binding constant (L/mg) corresponding to the maximum binding energy. A plot of qe against lnCe resulted into

Figure 10. The correlation coefficient (R^2 = 0.455) indicate that the Temkin Model does not fit the adsorption process. The Temkin isotherm parameters were calculated and summarized in Table 4.

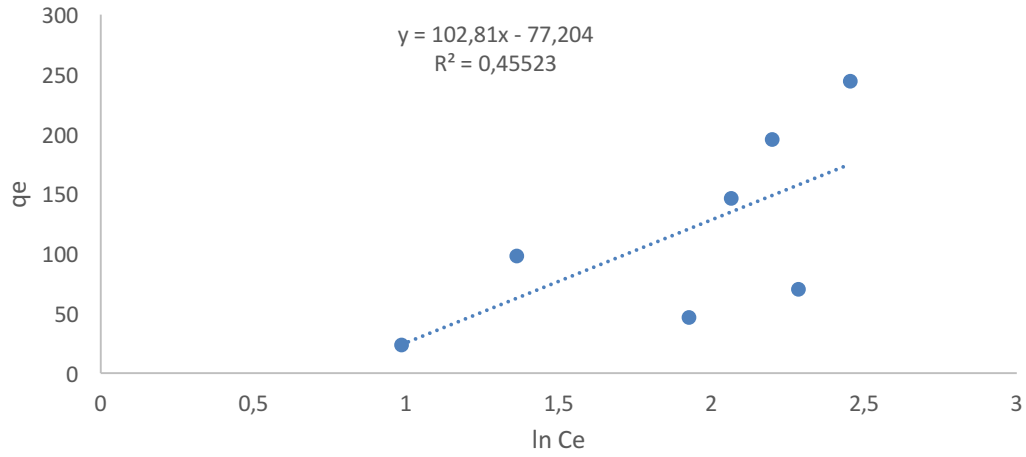

Figure 10. Temkin adsorption isotherm plots for adsorption of CV onto RCPH

Comparing the values of the correlation coefficient, R^2, for the three tested isotherms, it can be observed that the adsorption data fitted well to the Langmuir isotherm.

Table 4. Isotherm Constant for the adsorption of CV onto Raw Cowpea husk (R-CPH)

Langmuir			Freundlich				Temkin		
Q_{max}	K_L(L/mg)	R^2	1/n	n	K_f	R^2	A	B	R^2
153.85	0.049	0.907	0.710	1.4084	8.570	0.8764	0.472	102.81	0.455

3.5 Thermodynamics of the adsorption

Thermodynamic parameters give useful information about the nature of an adsorption process. The effects of temperature on the adsorption of CV onto R-CPH were studied by varying the temperature from 303 to 333K while keeping all other parameters at optimized values. The thermodynamic constants such as changes in free energy (ΔG), enthalpy (ΔH) and entropy (ΔS) give useful view about the feasibility and the spontaneous nature of the adsorption process and generally can be obtained from equations (18) and (19):

$$\Delta G = -RT \ln K_c \quad (18)$$

$$\ln K_c = -\Delta G/RT = -(\Delta H/RT) + (\Delta S/R) \quad (19)$$

Where R is the gas constant (8.314 J/molK), T is the absolute temperature (K), and K_c is the thermodynamic equilibrium constant and can be obtained from the relation in equation (20) [38]:

$$K_c = C_a/C_e \quad (20)$$

Where C_a is mg of CV adsorbed per liter and C_e is the equilibrium CV concentration of solution (mg/L). Both ΔH and ΔS were obtained from the slope and intercept of van't Hoff plot of $\ln K_c$ versus $1/T$.

Table 5. Thermodynamics Parameter of CV Adsorption onto Raw Cowpea Husk

T(K)	ΔG(kJ/mol)	ΔH (kJ/mol)	ΔS(J/mol.K)
303	-2789.69	264.78	-0.0141
313	-3318.95		
323	-4518.49		
333	-4459.32		

As can be observed in the **Table 5**, the positive value of ΔH indicates that the adsorption of the CV onto RCPH is endothermic in nature, and the adsorption occurs easily at higher temperature signifying a process of chemical adsorption. The negative ΔS indicate decreased randomness at the solid-liquid interface during adsorption of CV onto R-CPH [39]. The negative values of ΔG show the adsorption is thermodynamically feasible and spontaneous. Also, the ΔG value increase as the temperature increase (303 - 333) K.

Conclusion

An untreated cowpea husk adsorbent was employed to remove crystal violet dye from aqueous solution through a batch adsorption technique. The adsorbent was first characterized using FTIR and SEM methods, while relevant physical properties including density, moisture content and pore volume were determined. Three adsorption isotherm models were used to study the adsorption data obtained with Langmuir been the most favourable. Out of the four kinetic models tested, pseudo second order kinetics was found to fit well the kinetic data generated. The adsorption process was qualified to be spontaneous and feasible based on the thermodynamic parameters evaluated including enthalpy, entropy and Gibb's free energy. On the basis of the results obtained, it can be concluded that raw cowpea husk can efficiently be utilized as an adsorbent for the removal of crystal violet dye from aqueous solution at the studied conditions through the mechanism of chemical adsorption. As a waste product, it provides a solution for solid-waste management and solves the problem of its disposal and therefore, the reported study is an environmentally friendly method. For future studies, the usability of cowpea husk for dyes removal from real wastewater should be studied and as comparison, a fixed bed column be employed to investigate the effect of reactor design.

Acknowledgement

The authors wish to thank the technical staff of Chemistry Laboratory; Mal. Habibu, Mr. Joshua and Mal. Musa Beli for their co-operation in acquiring chemicals and guidance in the laboratory and also for their willingness and readiness to assist at all times during this work.

Conflict of Interest

The authors declare that the research was conducted in the absence of any commercial or financial relationships that could be construed as a potential conflict of interest.

References

[1] E. Rápó, L. E. Aradi, A. Szabó, K. Posta, R. Szep, S. Tonk, Adsorption of remazol brilliant violet-5R textile dye from aqueous solutions by using eggshell waste biosorbent. *Sci Rep* 10**,** 8385 (2020). https://doi.org/10.1038/s41598-020-65334-0.

[2] A. Alhujaily, H. Yu, X. Zhang, F. Ma, Adsorptive removal of anionic dyes from aqueous solutions using spent mushroom waste. *Appl Water Sci* 10**,** 183 (2020). https://doi.org/10.1007/s13201-020-01268-2.

[3] A. M. Abbas, F. H. Abdulrazzak, W. J. Sabbar, R. A. Faraj, Adsorption of dyes by activated carbon surfaces were prepared from plant residues, A Review *J. Mater. Environ. Sci.,*11: 2007-2015 (2020).

[4] P. P. Ndibewu, C. M. Kede, P. G. Tchieta, H. Z. Poumve, A. N. Tchakounte, Simultaneous adsorption of mercury (ii) and zinc (ii) ions from aqueous solution onto activated carbons derived from a lowland bioresource waste, *J. Appl. Surf. Interphase* 5(1-3): 21-30 (2019).

[5] C.O. Ania, F. Beguin, Mechanism of adsorption and electrosorption of bentazone on activated carbon cloth in aqueous solutions, *Water Res.* 41: 3372–3380 (2007).

[6] V. Arora, D. P. Tiwari, Analysis of adsorptive characteristics of chemically modified bio-waste walnut shell for degradation of brilliant yellow dye, Appl. *J. Envir. Eng. Sci.* 5(3): 23 1-240 (2019). https://doi.org/10.48422/IMIST.PRSM/ajees-v5i3.15585.

[7] D. Ma, S. Zhang, S. Zhan, L. Feng, S. Zeng, Q. Lin, Y. Pan, Adsorptive removal of catechol from aqueous solution with a water stable and hydroxyl functionalized terbium-organic framework, *Ind. Eng. Chem. Res*. 58(43): 20090-20098 (2019). https://doi.org/10.1021/acs.iecr.9b05067.

[8] B. Idoko, A. A. Mohammed, Adsorption of Congo red dye from aqueous solution by carbonised cowpea (V*igna Unguiculata*) husk: Kinetics, equilibrium and thermodynamics studies, *Journal of Experimental Research,* 8(2):1-9 (2020).

[9] A. M. Ayuba and B. Idoko, Kinetic, equilibrium and thermodynamic studies on the adsorption of crystal violet dye from aqueous solution using activated cowpea (*Vigna Unguiculata)* husk, *Applied Journal of Environmental Engineering Sciences,* 6(2): 182-195 (2020).

[10] E. Sebata, M. Moyo, U. Guyo, N. P. Ngano, B. C. Nyamunda, F. Chigondo, M. S. Chitsa, Adsorptive removal of Atrazine from aqueous solution using Bambara groundnut hulls. *International Journal of Engineering Research & Technology*, 2(5): 312 – 321 (2013).

[11] T. Nharingo, N.M. Muzondo, E. Madungwe, F. Chigondo, U. Guyo, and B. Nyamunda, Isotherm Study of the biosorption of Cu (II) from aqueous solution by *Vigna subterranean* (L.) verdc hull. *International Journal of Scientific and Technology Research*, 2(4): 199 – 206 (2013).

[12] N. Abdus‑Salam, and S. K. Adekola, Adsorption studies of zinc (II) on magnetite, baobab (*Adansonia digitata*) and magnetite–baobab composite *Applied Water Science*, 28-222 (2018). https://doi.org/10.1007/s13201-018-0867-7

[13] A. D. N'diaye, M. Sid'A. Kankou, Adsorption of aspirin onto biomaterials from aqueous solutions *J. Mater. Environ. Sci.,*11: 1839-1845 (2020).

[14] A. D. N'diaye, M. S. Kankou*, S*orption of caffeine onto low cost sorbent: application of two and three-parameter isotherm models, *Appl. J. Envir. Eng. Sci*. 5(3): 263-272 (2019). https://doi.org/10.48422/IMIST.PRSM/ajees-v5i3.17210.

[15] AOAC *Official Methods of Analysis.* AOAC International Washington D.C 17th Edn, 1456-1500 (2005).

[16] F. A. Ugbe and N. Abdus-Salam, Kinetics and thermodynamic modelling of natural and synthetic goethite for dyes scavenging from aqueous systems, *Arabian Journal of Chemical and Environmental Research*, 7(1): 12–28 (2020).

[17] A. M. Ayuba and T. A. Nyijime, Kinetic and equilibrium studies of paraquat dichloride adsorption on raw Bambara groundnut (*Vigna subteranean*) shells. *Appl. J. Envir. Eng*. Sci. 6 (1): 1-13 (2020).

[18] A. A. Muhammad and N. T. Aondofa, Paraquat dichloride adsorption from aqueous solution using carbonized Bambara groundnut (*Vigna subterranean*) shells, *Bayero Journal of Pure and Applied Sciences*, 12(1): 167 – 177 (2019).

[19] E. J. Inam, J. B. Edet, P. E. Akpan, K. E. Ite, Characterization and equilibrium studies for the removal of methylene blue from aqueous solution using activated bone char. *J. Mater. Environ. Sci.,* 11: 167-1675 (2020).

[20] S. Chowdhury, R. Mishra, P. Saha, P. Kushwaha, Adsorption thermodynamics, kinetics and isosteric heat of adsorption of malachite green onto chemically modified rice husk. *Desalination* 265:159–168 (2011). doi:10.1016/j.desal.2010.07.047

[21] H. Ali, N. Mladenka, I. Mihajlović, Sorption of carbendazim and linuron from aqueous solutions with activated carbon produced from spent coffee grounds: Equilibrium, kinetic and thermodynamic approach, *Journal of Environmental Science and Health*, Part B, (2018) DOI: 10.1080/03601234.2018.1550307.

[22] M. R. Sagir, A. M. Ayuba, U. Umar, S. Y. Mohammed, M. Kabir, H. Suleiman, M. Abubakar, T. A. Danmusa, Thermodynamics study of Congo red dye adsorption onto H_2SO_4 treated rice husk

(*Oryza sativa*) powder. *Dutse Journal of Pure and Applied Sciences (DUJOPAS),* 6(4): 113-119 (2020).

[23] A. D. N'diaye, M. Sid'A. Kankou, Sorption of caffeine onto low-cost sorbent: Application of two and three-parameter isotherm models. *Appl. J. Envir. Eng. Sci.* 5(3): 263-272 (2019).

[24] T. A. Nguyen, V. T. Nguyen, T. T. Hieu Tran, T. Q. Nhu Le, N. H. Nguyen, Batch and column adsorption of reactive dyes by eggshell powder–chitosan gel core-shell material. *Mor. J. Chem*. 9(1): 018-027 (2021).

[25] A. Bayu, D. Nandiyanto, Isotherm adsorption of carbon microparticles prepared from Pumpkin (*Cucurbita maxima*) seeds using two-parameter monolayer adsorption models and equations. *Mor. J. Chem.* 8(3): 745-761 (2020).

[26] N. Gupta, A. K. Kushwaha, M. C. Chattopadhyaya, Adsorption studies of cationic dyes onto Ashoka (*Saraca asoca*) leaf powder, *J Taiwan Inst Chem Eng* 43:604–613 (2012). doi:10.1016/j.jtice.2012.01.008.

[27] A. M. Ayuba, M. Ladan, A. S. Muhammad, Thermodynamic and kinetic study of Pb(II) amputation by river sediment. *Appl. J. Envir. Eng. Sci*. 6(3): 213-226 (2020).

[28] I. A. Nnanwube, O. D. Onukwuli, V. N. Okafor, J. I. Obibuenyi, R. O. Ajemba, C. C. Chukwuka, Equilibrium, kinetics and optimization studies on the bleaching of palm oil using activated Karaworo kaolinite. *J. Mater. Environ. Sci.,* 11: 1599-1615 (2020).

[29] W. J. Weber, J. C. Morris, Kinetics of adsorption on carbon from solution. *J. Sanit. Eng. Div. Proc. Am. Soc. Civil. Eng.* 89, 31–59 (1963).

[30] I. Langmuir, The adsorption of gases on plane surfaces of glass, mica and platinum, *J. Am. Chem. Soc*. 40, 1362-1403 (1918).

[31] B. H. Hameed and M. I. El-Khaiary, Malachite green adsorption by Rattan sawdust: isotherm, kinetic and mechanism modelling, *Journal of Hazardous Materials,* 159: 574–579 2008.

[32] N. Oubna, M. Youssef, A. Ouissal1, EL B. Aziz1, EL K. Bouchta, Z.Farid, Kinetic and thermodynamic study of the adsorption of two dyes: brilliant green and eriochrome black T using a natural adsorbent sugarcane bagasse, *Mor. J. Chem.* 7(4): 715-726 (2019).

[33] Q. Husain, Peroxidase mediated decolorization and remediation of wastewater containing industrial dyes: a review. *Reviews in Environmental Science and Bio/Technology*, *9*(2): 117-140 (2010).

[34] H. Freundlich, *Colloid and capillary chem*. Metheum. London, (1926).

[35] C. Jude, F. C. Igwe, A. A. Augustine, Kinetics and equilibrium isotherms of pesticides adsorption onto boiler fly ash. *Terrestrial and aquatic environment toxicology, global science books,* 6(1): 21-29 (2012).

[36] G. O. Achieng, V. O. Shikuku, Adsorption of copper ions from water onto fish scales derived

biochar: Isothermal perspectives. *J. Mater. Environ. Sci.,*11: 1816-1827 (2020).

[37] M. I. Temkin, V. Pyzhev, Kinetics of ammonia synthesis on promoted iron catalyst, *Acta Phys. Chim. USSR 12,* 327–356 (1940).

[38] N. Hassan, A. Shahat, A. El-Didamony, M. G. El-Desouky, A. A. El-Bindary, Equilibrium, Kinetic and Thermodynamic studies of adsorption of cationic dyes from aqueous solution using ZIF-8. *Mor. J. Chem.* 8(3): 627-637 (2020).

[39] A. Machrouhi, M. Farnane, A. Elhalil, M. Abdennouri, H. Tounsadi, N. Barka, Heavy metals biosorption by *Thapsiatran stagana* stems powder: Kinetics, equilibrium and thermodynamics. *Mor. J. Chem*. 7(1): 098-110 (2019).

(2021) ; www.mocedes.org/ajcer